Structural Engineering and Mechanics, Vol. 20, No. 4 (2005) 421-434
DOI: http://dx.doi.org/10.12989/sem.2005.20.4.421

Numerical studies on the effects of the lateral boundary on soil-structure interaction in homogeneous soil foundations

Z. N. Li†

College of Civil Engineering, Hunan University, Changsha, Hunan, 410082, China
College of the Architectural and Civil Engineering, Wenzhou University, Wenzhou, 325027, China

Q. S. Li‡

Department of Building and Construction, City University of Hong Kong, 83 Tat Chee Avenue, Kowloon, Hong Kong, China

M. L. Lou†

State Key Laboratory for Disaster Reduction in Civil Engineering, Research Institute of Structural Engineering and Disaster Reduction, Tongji University, Shanghai 200092, China

(Received July 22, 2004, Accepted April 1, 2005)

Abstract. In this paper, the finite element method is applied to investigate the effect of the lateral boundary in homogenous soil on the seismic response of a superstructure. Some influencing factors are presented and discussed, and several parameters are identified to be important for conducting soil-structure interaction experiments on shaking tables. Numerical results show that the cross-section width L, thickness H, wave propagation velocity and lateral boundaries of soil layer have certain influences on the computational accuracy. The dimensionless parameter L/H is the most significant one among the influencing factors. In other words, a greater depth of soil layer near the foundation should be considered in shaking table tests as the thickness of the soil layer increases, which can be regarded as a linear relationship approximately. It is also found that the wave propagation velocity in soil layer affects the numerical accuracy and it is suggested to consider a greater depth of the soil layer as the wave propagation velocity increases. A numerical study on a soil-structure experimental model with a rubber ring surrounding the soil on a shaking table is also conducted. It is found the rubber ring has great effect on the soil-structure interaction experiments on shaking table. The experimental precision can be improved by reasonably choosing the elastic parameter and width of the rubber ring.

Key words: soil-structure interaction; finite element method; earthquake engineering; shaking table test.

† Professor
‡ Associate Professor, Corresponding author, E-mail: bcqsli@cityu.edu.hk

1. Introduction

The soil-structure interaction in earthquake engineering has been studied extensively over the last three decades. The key problem related to soil-structure interaction is how to deal with the infinite half space of soil medium. Because the analytical or semi-analytical solutions for soil-structure interaction based on the wave theory is very limited, numerical methods combining the finite element method with the infinite element method or the infinite mapping technique with various virtual boundary conditions have been developed for solving various kinds of complicated soil-structure interaction problems (Liu *et al.* 2004, Dominguez 1978, Lysmer and Kulemeyer 1969, Liao 1987, Zhang 1991, Lou and Liu 1986, Lou *et al.* 2000). Genes and Kocak (2002) studied the large-scale soil-structure interaction system by the finite element method with the scaled boundary-finite elements and it was found that the computation time was much saved for such a large-scale problem. Aviles and Suarez (2002) determined the effective periods and damping of building-foundation systems considering seismic wave effects. Kocak and Mengi (2000) developed a relatively simple three-dimensional soil-structure interaction model and exhibited good numerical performance comparing with other existing methods. Recently, Huang *et al.* (2003) presented a study on numerical modeling of shear occurring along a soil-structure interface. Anandarajah *et al.* (1995) examined the pile-soil-structure interaction of a two-storey building under earthquake excitation through a series of model experiments and numerical analysis using the finite element method. It was found that the numerical results agreed well with the experimental data. Since it is usually difficult to conduct experimental works on soil-structure interaction, researches on this topic have been mainly concentrated on numerical simulation and relatively less work has been done on model tests. Furthermore, there was a lack of study carried out on how to determine the range of soil layer required in model tests on shaking tables and how to adopt suitable far-field boundaries to improve the experimental precision. Such problems will be studied in this paper.

Generally, if the damping of soil is ignored, it is believed that the virtual lateral boundaries after truncating the horizontal soil layer may result in the elastic wave reflection and its effect can not be underestimated. However, in actual soil medium, the soil damping may absorb the wave energy and weaken the wave reflection effect from the lateral boundaries. Influence of various locations of lateral boundaries on the ground dynamical flexibility was discussed by Lou and Lin (1986) in which the behavior of foundation was assumed to be linear viscoelastic. Quantitative relationship between the lateral boundary location and the reflection effect was also given in their study. In this paper, the effects of the lateral boundaries in homogenous soil on the seismic response of a superstructure are numerically investigated. The outputs of this study can provide not only the valuable information for numerical analysis of soil-structure interaction, but also the guidelines for selecting the range of soil layer required in soil-structure interaction model test on shaking tables.

2. Numerical models

Fig. 1 shows the analytical model for soil-structure interaction including the two-dimensional homogenous soil layer and a superstructure simplified as a single degree of freedom (SDOF) system. The structure is built on the massless foundation with width b which is fully uncovered on the ground. The rigid foundation is perfectly bonded to the surrounding soil. The natural frequency of vibration ω_c of the SDOF system representing the superstructure can be adjusted by varying the

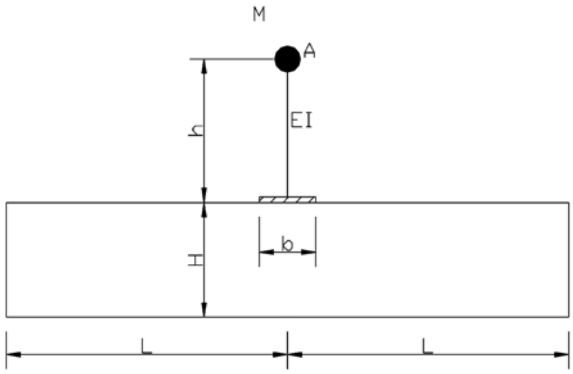

Fig. 1 The model for analyzing soil-structure interaction

parameters M and EI. The fundamental frequency of shearing vibration in the horizontal direction of the soil medium can be determined by

$$\omega_s = \frac{\pi v_s}{2H} \tag{1}$$

where v_s and H are the shear wave propagation velocity and thickness of the soil layer, respectively.

In this paper, the finite element method is used to study the seismic response of the finite layered soil-structure system. Two types of elements are adopted: one is the 4-noded plane element for the discretization of the layered soil layer; the other is the beam element for the superstructure. The global discrete equations of motion of the soil-structure system can be expressed as

$$[M]\{\ddot{u}(t)\} + [C]\{\dot{u}(t)\} + [K]\{u(t)\} = -[M]\{e\}\ddot{u}_g(t) \tag{2}$$

where $\{u(t)\}$ is the displacement vector of the soil-structure system relative to the base rock; $[M]$, $[C]$ and $[K]$ are the global mass, damping and dynamical-stiffness matrices, respectively; $\ddot{u}_g(t)$ denotes the ground earthquake excitation and $\{e\}$ is a matrix with diagonal elements of one and other elements of zero.

Considering the connection requirements between the plane 4-noded element and beam element, coordinate transformation between nodes on the rigid foundation can be built up. As an example, the rigid foundation is assumed to cover two plane elements as shown in Fig. 2. The nodal coordinate transformation matrix can be obtained accordingly in this case. Detailed procedures are given below.

The nodal displacement components at the end of the beam are defined as $(\overline{u}_j, \overline{v}_j, \theta_j)$ and the associated nodal displacements of the quadrilateral element are $(u_i, v_i, u_j, v_j, u_k, v_k)$. According to the perfect bonding requirements between the rigid foundation and soil layer, the following six constraint conditions are obtained:

$$u_i = u_j = u_k = \overline{u}_j \tag{3a}$$

$$v_j = \overline{v}_j, \quad v_i = \overline{v}_j - l_i\theta_j, \quad v_k = \overline{v}_j + l_k\theta_j \tag{3b}$$

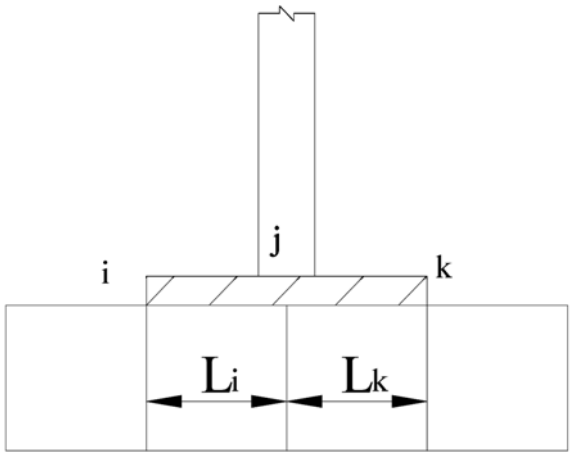

Fig. 2 The connections between the structure and soil

Thus, only 3 nodal degrees of freedom are independent among the total 9 nodal displacement components. Selecting $(\overline{u}_j, \overline{v}_j, \theta_j)$ as independent ones, one has the following nodal coordinate transformation matrix at the joint.

$$\begin{Bmatrix} \overline{u}_j \\ \overline{v}_j \\ \theta_j \\ u_i \\ v_i \\ u_j \\ v_j \\ u_k \\ v_k \end{Bmatrix} = \begin{bmatrix} 1 & 0 & 0 \\ 0 & 1 & 0 \\ 0 & 0 & 1 \\ 1 & 0 & 0 \\ 0 & 1 & -l_i \\ 1 & 0 & 0 \\ 0 & 1 & 0 \\ 1 & 0 & 0 \\ 0 & 1 & l_k \end{bmatrix} \begin{Bmatrix} \overline{u}_j \\ \overline{v}_j \\ \theta_j \end{Bmatrix} = [T] \begin{Bmatrix} \overline{u}_j \\ \overline{v}_j \\ \theta_j \end{Bmatrix} \tag{4}$$

Note that the two other adjacent rectangular elements are affected by the coordinate transformation besides the two elements directly bonded with the rigid foundation. Therefore, total 4 elements as shown in Fig. 2 need to be considered. One can obtain the modified elemental stiffness matrices of these four elements one by one after introducing the transformation relationship as given in Eq. (4). Finally, the global discrete equations of motion of the soil-structure system are revised after assembling all the elements:

$$[\overline{M}]\{\ddot{u}(t)\} + [\overline{C}]\{\dot{u}(t)\} + [\overline{K}]\{u(t)\} = -\{\overline{P}(t)\} \tag{5}$$

where

$$[\overline{M}] = [T]^T[M][T] \tag{6a}$$

$$[\bar{C}] = [T]^T[C][T] \tag{6b}$$

$$[\bar{K}] = [T]^T[K][T] \tag{6c}$$

$$\{\bar{P}(t)\} = [T]^T\{P(t)\} = -[T]^T[M]\{e\}\ddot{u}_g(t) \tag{6d}$$

In case more quadrilateral elements are directly jointed with the rigid foundation, the corresponding coordinate transformation can be obtained similarly.

In order to examine the effect of the virtual lateral boundaries, the relative errors of the maximum amplitudes of displacement and acceleration at the point A shown in Fig. 1 are considered in this paper. The relative error of amplitude of vibration is defined as:

$$e = \frac{a_{in} - a_\infty}{a_\infty} \tag{7}$$

where a_{in} and a_∞ are the peak values of vibration considering finite domain and infinite half space of soil layer, respectively. In the present computation, a_∞ is obtained using Eq. (5) provided that the lateral boundary is sufficiently far away from the rigid foundation. Numerical tests with various locations of the lateral boundaries are conducted to assure the stability and reliability of the results. For instance, we can compute two peak values of vibration of the superstructure for two locations of the lateral boundaries, i.e., $L/b = N$ and $L/b = N - 1$. Comparing the two values, one can establish the virtual viscous damping boundary at the latter location once the relative error is less than a certain value (for example, 1%).

The viscous damping boundary condition (Liao 1987) is given here:

$$\sigma(t) = \rho v_p \dot{u}(t), \text{ in the horizontal direction} \tag{8a}$$

$$\tau(t) = \rho v_s \dot{v}(t), \text{ in the vertical direction} \tag{8b}$$

Note that only an additional diagonal damping matrix is needed in Eq. (5) after considering the viscous damping boundary (Li *et al.* 1998). The equation forms and computational procedures are not affected. The corresponding solutions of the structural responses using the above technique are regarded as "exact values" in this paper.

3. Influences of various parameters

The relative error of dynamic response of the simplified soil-structure interaction system as shown in Fig. 1 can be computed by Eq. (7) as mentioned in the previous section. It is a function of multiple parameters, such as, the natural frequency of vibration of the superstructure ω_c, mass M, height of the superstructure h, wave propagation velocity v_s and thickness H of the soil layer, damping ratio β of the soil medium and the rigid foundation width b. Thus, we have

$$e = e(\omega_c, \omega_s, h, H, b, v_s, \beta, \ldots) \tag{9}$$

It is well known that the earthquake propagation wave is composed of multiple frequency

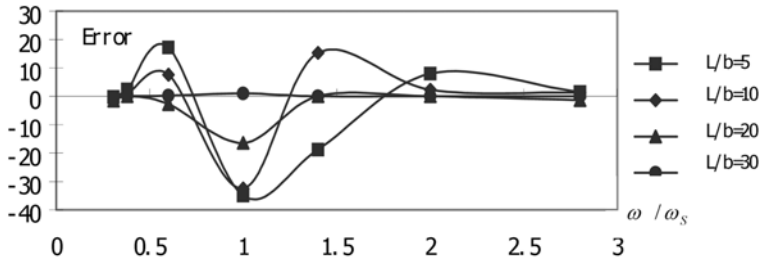

Fig. 3 The relative error of the acceleration response at point A under the sinusoidal wave considering various locations of the lateral boundary ($\omega_c/\omega_s = 0.5$)

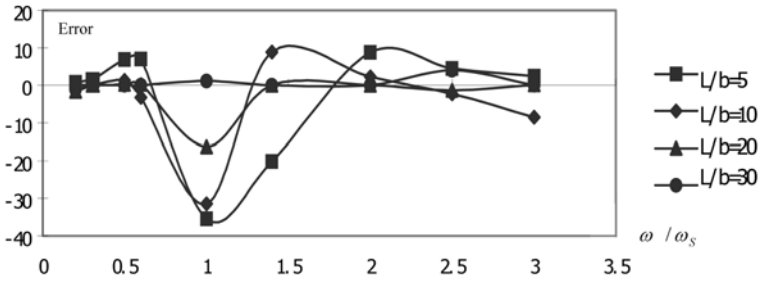

Fig. 4 The relative error of the acceleration response at point A under the sinusoidal wave considering various locations of the lateral boundary ($\omega_c/\omega_s = 2.0$)

characteristics and is time-dependent. In the linear condition, the total seismic response of a structural system can be regarded as the summation of the dynamical response under every harmonic component within the seismic wave. Therefore, in the present computation, the input seismic wave acting on the bottom of the soil layer is assumed to be a sinusoidal wave with amplitude of 0.2 g. It is noticed that the relative error e of the structural response is not dependent on the amplitude of the input seismic wave for a linear elastic system.

In this paper, the shear wave propagation velocity and thickness of the soil layer are taken to be $v_s = 350$ m/s and $H = 30$ m, respectively. Various ranges of the finite soil layer with $L/b = 5$, 10, 20 and 30 are considered in the computation. Figs. 3 and 4 show the relative errors of the acceleration response at point A under the sinusoidal wave with various frequency values of ω. Note that in Fig. 3 the natural frequency of the superstructure is lower than that of soil with $\omega_c/\omega_s = 0.5$. On the contrary, Fig. 4 shows the case that the natural frequency of the superstructure is greater than that of soil with $\omega_c/\omega_s = 2.0$. In the computation, we take: h = 100 m, b = 20 m.

It is observed from Figs. 3 and 4 that $|e|$ reaches the maximum value when ω/ω_s is close to 1. It is also found that the maximum value of $|e|$ is achieved as ω/ω_s tends to unity even when the shear wave propagation velocity of the soil layer approaches to 150 m/s. Similar conclusion can be drawn when the thickness of the soil layer varies. Therefore, we will investigate the relative error of the structural response under this input frequency ω/ω_s hereafter.

3.1 Effect of the relative thickness H/b and shear wave propagation velocity of soil layer

Fig. 5 shows the variations of the relative error of the acceleration response at point A with the

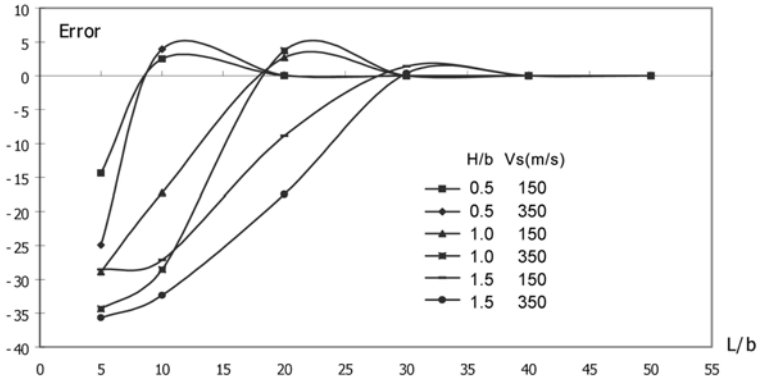

Fig. 5 Effect of L/b on the relative error e

dimensionless locations L/b where the lateral boundaries are installed. Various sets of the relative thickness H/b and shear wave propagation velocity v_s of the soil layer are considered. In case $v_s = 150$ m/s, it is found that the relative error $|e|$ is less than 5% for $H/b = 0.5$, $L/b \geq 8$; $H/b = 1.0$, $L/b \geq 15$; and $H/B = 1.5$, $L/b \geq 23$. In case $v_s = 350$ m/s, it is observed that the larger value of L/b is required to assure the relative error $|e|$ less than 5%. This illustrates that larger range of soil layer needs to be taken in shaking table tests as the thickness of soil layer increases.

3.2 Effect of the parameter L/H

The same data presented in Fig. 5 are rearranged by setting the parameter L/H as the horizontal coordinate as shown in Fig. 6. It is seen from Fig. 6 that the effects of H/b and v_s on the relative error e can be ignored in comparing with those of L/H. The relationship between e and L/H can be clearly observed and fitted. For example, to ensure $|e|$ less than 5%, the soil layer range with $L/H = 7$~9 is required; while for the case of $|e|$ less than 10%, only $L/H = 6$~8 is sufficient.

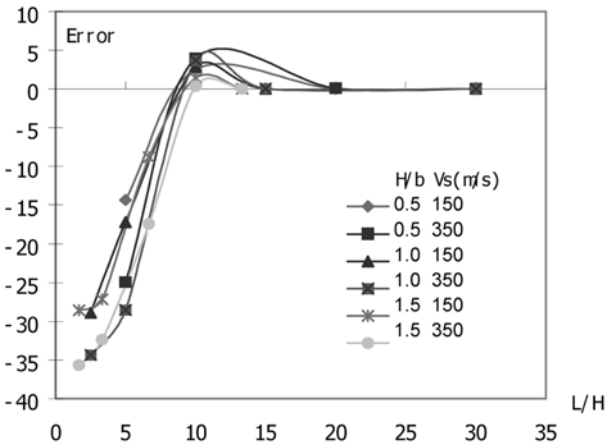

Fig. 6 Effect of L/H on the relative error

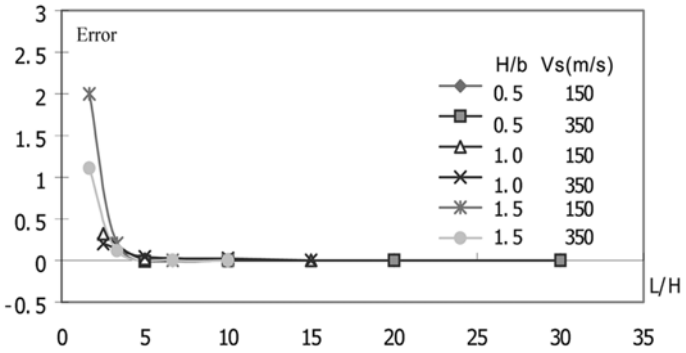

Fig. 7 The relative error when the soil-structure system resonates

3.3 Effect of the structural resonance

When the natural frequency of the superstructure is lower than that of the soil medium ($\omega_c < \omega_s$), it is found that the structural system resonates with the largest response when the frequency of the input sinusoidal wave is close to the natural frequency of the soil-structure system. Fig. 7 shows the relative error caused by truncating the infinite soil layer into the finite domain layer when the soil-structure system resonates. However, it is shown from Fig. 7 that the error of the relative acceleration response is relatively small when the frequency of the input sinusoidal wave is equal to the natural frequency of the system. In general, e is less than 5%.

It is known that the natural frequency ω_0 of the soil-structure system is usually lower than that of the superstructure ω_c, i.e., $\omega_0 < \omega_c$. In this case with $\omega_0/\omega_c < 1$, it is found that the value of e is not the largest as shown in Fig. 3. Comparing the results presented in Fig. 7 and those plotted in Figs. 5 and 6, it is found that the computational error duo to take the finite soil layer is the upper bound in Figs. 3-6. In other words, the dimensionless parameter L/H is the most significant one among the influencing factors. Fig. 7 also shows that the effect of H/b on e is much less than that of L/H.

3.4 Effect of the height of the concentrated mass

As shown in Fig. 8, the effect of h/b on e is much less than that of v_s. Generally speaking, the

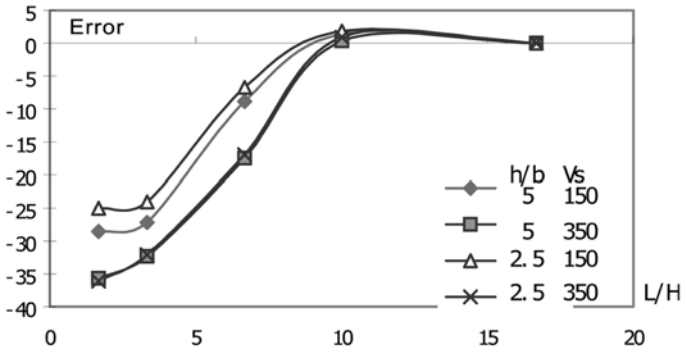

Fig. 8 The effect of h/b on the relative error e

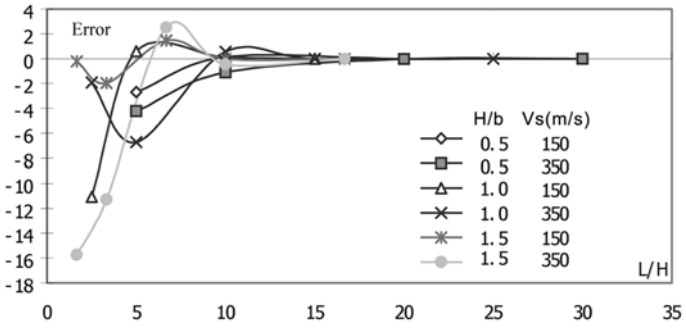

Fig. 9 The relative error with the input as the EL Centro record

relative error increases as the shear wave propagation velocity of the soil layer becomes larger. Here we assume the natural frequency of the superstructure is fixed.

3.5 Effect of earthquake excitations

Fig. 9 shows the relative error with the input selected as the EL Centro earthquake record. It is noticed that the effect of H/b and v_s on e can be ignored in contrast with that of L/H. It is also clearly found that the relative error with the EL Centro record is much smaller than that with the sinusoidal waves. However, its variation is relatively complex. Therefore, it is concluded that that the relative error caused by the input sinusoidal waves is the upper bound. That is why we select the sinusoidal waves as the earthquake excitation inputs in this study.

3.6 Effect of damping ratio

In the present computations, the damping ratios ξ for the structure and ξ_g for soil material are adopted as 0.035 and 0.08, respectively. According to Wolf's study (1985), the equivalent damping ratio $\bar{\zeta}$ of a soil-structure interaction system is about 0.2 ($\bar{\zeta} \to 0.2$) when $\bar{S} > 1$ and $H/b \geq 1$, in which $\bar{S}$ is the stiffness ratio of the structure and of the soil and $\bar{S} = \omega_c h/v_s$ (ω_c is the fixed-base frequency of the structure, v_s is the shear wave velocity and h is the height of the structure). In other words, once $\bar{S} > 1$ and $H/b \geq 1$ is satisfied, the equivalent damping ratio varies in a very small range and its value tends to be 0.2. Since the equivalent damping ratio can be regarded as a constant in the cases always encountered in engineering practices, there will be no further discussion about its effect on the computational errors in this study.

4. Effect of the rubber ring in model tests on shaking tables

In numerical simulation of soil-structural interaction under seismic excitation, one can select adequate range of soil layer or artificial lateral boundaries to control and reduce the numerical error as discussed in the previous section. However, it is inevitable to truncate the finite range of soil layer in the soil-structural interaction model tests on shaking tables. The available selection range is very limited due to the bearing capacity of shaking tables. Therefore, it is necessary to reduce the experimental error caused by taking the finite soil layer in this kind of model tests. Currently,

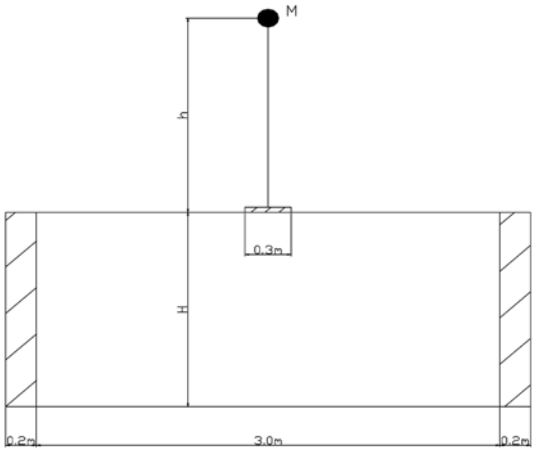

Fig. 10 The sketch of the soil-structure model test on a shaking table with the rubber ring

circular rubber ring or cylinder with certain thickness is usually adopted to be the container of the finite soil layer (Lou *et al*. 2000). Fig. 10 shows an example with the cross-section at the diameter location of such a rubber ring. With the plane strain assumption, the effect of the rubber ring on the accuracy of the model test is numerically examined using this example.

In this example, the shear wave propagation velocity of the soil layer is kept to be 150 m/s, while the soil layer thickness is assumed to be 1.5 m or 0.75 m. The concentrated mass is taken to be 450 kg or 45 kg. Variation of the shearing modulus of the rubber ring is considered to study its influence. It is taken to be 6.7×10^x MPa in this study where x is a variable. In the finite element discretization of the rubber ring, only one element is used along the horizontal direction. In the height direction, the division is consistent with the soil layer. Two kinds of constraints are adopted for the nodes at the rubber ring. One is free so that the node can deform arbitrarily; the other is that the vertical nodal degree of freedom is fixed so that the node can only have horizontal deformations. It is also required for the latter constraint that only shearing deformation is permitted. Figs. 11-14 show the variations of the relative errors of the acceleration response at the top of the superstructure with the shearing modulus of the rubber ring. Note that the power x in the shearing

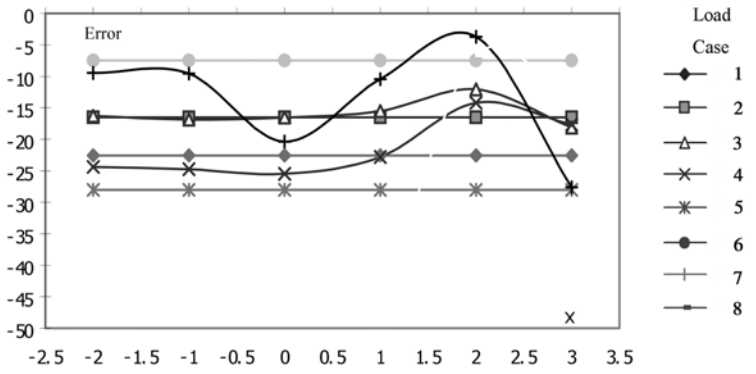

Fig. 11 Comparison of the relative errors with and without the rubber ring (H = 0.75 m, h = 1.5 m)

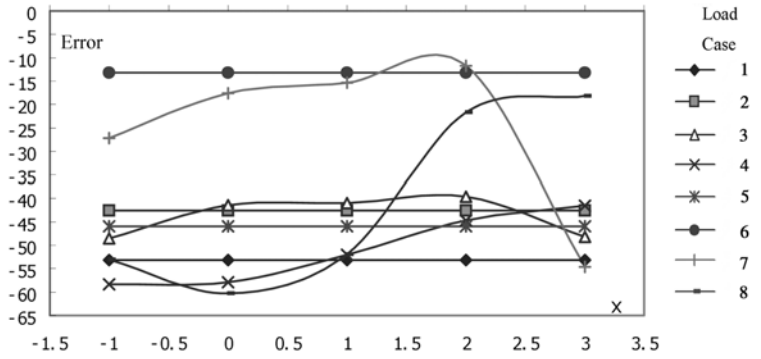

Fig. 12 Comparison of the relative errors with and without the rubber ring (H = 0.75 m, h = 0.5 m)

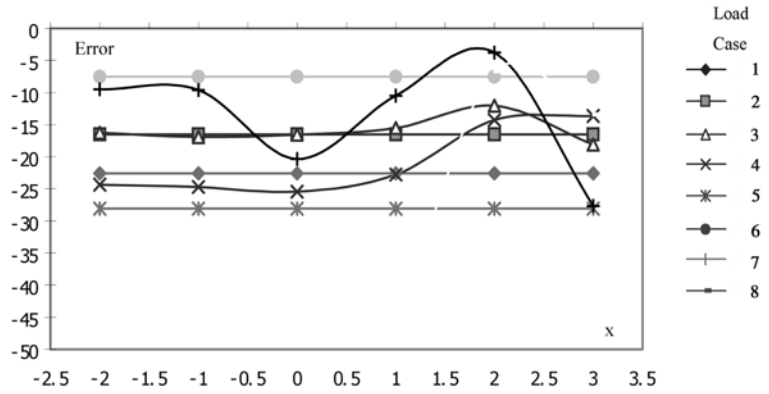

Fig. 13 Comparison of the relative errors with and without the rubber ring (H = 1.5 m, h = 1.5 m)

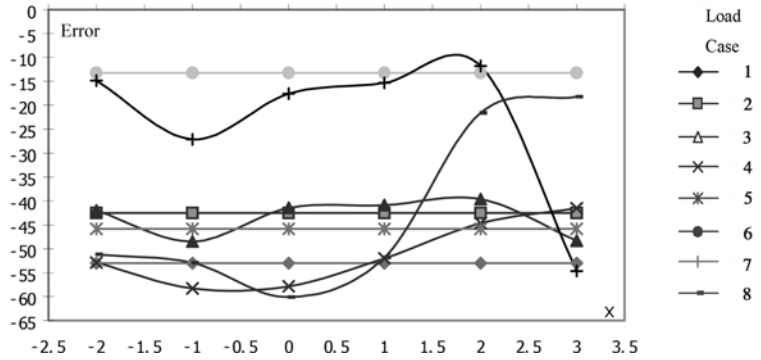

Fig. 14 Comparison of the relative errors with and without the rubber ring (H = 1.5 m, h = 0.75 m)

modulus 6.7×10^x MPa is taken as the horizontal coordinate and the relative error as the vertical coordinate in these figures.

In Figs. 11-14, various loading cases are considered as explained below.

Load case 1: M = 450 kg, no rubber ring, the lateral boundary nodes at the soil layer are totally free.

Load case 2: $M = 450$ kg, no rubber ring, the vertical deformations of the lateral boundary nodes at the soil layer are not allowed.

Load case 3: $M = 450$ kg, with the rubber ring, the vertical deformations of the lateral boundary nodes at the rubber ring are not allowed.

Load case 4: $M = 450$ kg, with the rubber ring, the lateral boundary nodes at the rubber ring are totally free.

Load cases 5 to 8 are corresponding to the cases 1 to 4, but the concentrated mass is replaced with $M = 45$ kg.

In case of no rubber ring surrounding the soil layer, it is found from the figures that the relative error of the acceleration response increases as the soil layer thickness increases provided that the soil layer has a fixed length in the horizontal direction. For example, comparing the results in Figs. 11-14 for the load case 6, the relative error e has the values of 7.5% and 14% when $H = 0.75$ m and $H = 1.5$ m, respectively. The vertical constraint of the lateral boundary nodes has certain influence on the relative error of the structural response. This can be observed by comparisons of the load cases 1 and 2, 5 and 6 in the figures. The relative error can be improved significantly by enforcing the vertical constraint of the lateral boundary nodes, especially when the concentrated mass is lighter. With addition of the rubber ring, it is found that the shearing modulus of the rubber has significant effect on the relative error e. In general, the relative error e becomes larger when the rubber ring with low shearing modulus is used under the same boundary conditions. Comparing the load case 3 with 4 or the load case 7 with 8 at about $x = 2.0$, it can be seen that the vertical constraint at the boundaries of the rubber ring reduces the relative error e to a great extent. Meanwhile, it is found that the relative error e is relatively small for the rubber with high shearing modulus even if no constraints are enforced at the boundaries of the rubber ring.

The computation error will increase if rubber rings with low shear modulus are added in the system when the same boundary conditions are applied. It is shown from the cases 3 and 7 that the computational error can be reduced significantly when vertical constrains are applied to the nodes of rubber rings at about $x = 2.0$. When rubber rings have relative high values of shear modulus, the relative error is very small even if no boundary constraints are applied to the nodes of rubber rings in the cases 4 and 8. This observation is very useful in the design of the soil-structure interaction model test on shaking tables. Actually, after the finite domain of soil layer is adopted, the effects of the ignored far field soil on the soil-structure interaction system exhibit in the following aspects:

a) The frequency characteristics of soil, especially its fundamental natural frequency, are altered. Therefore, larger range of soil is needed to assure the frequency characteristics especially those of the lower modes to be consistent with those of infinite half space domain soil layer.

b) The radiation damping is ignored due to the existence of larger material damping of the soil medium under vibration. Its effect is not significant in the elastic problems when the finite soil layer reaches a certain range.

c) The elastic constraint between the far field soil and the near field one is neglected which also affect the frequency characteristics of the soil layer. The rubber ring can compensate the elastic constraint effect to a certain extent when the shearing modulus of the rubber is higher than that of the soil layer.

d) When $\overline{S} > 1$ and $H/b \geq 1$, the seismic response of a structure is very close to that for the case of half-space soil layer (Wolf 1985). That is to say, when the soil layer depth meets $H/b \geq 1$, the variation of the computational results is not significant even if the soil layer depth increases.

5. Conclusions

In this paper, the finite element method is applied to numerically study the effect of truncating the infinite soil layer into the finite domain on the seismic responses of a superstructure. The outputs of this study provide not only the valuable information for numerical analysis of soil-structure interaction, but also the guidelines for selecting the range of soil layer required in the soil-structure interaction model test on shaking tables.

Major conclusions are drawn in the following.

a) The dimensionless parameter L/H is the most significant one among the influencing factors since it basically reflects the relationship of geometry proportion. In order to control the error in a certain level, larger range of soil layer should be considered as the soil layer thickness increases, which can be regarded as a nearly linear relationship.
b) The shearing wave propagation velocity of soil medium has certain effects. In other words, in case of higher speed of the wave propagation larger range of finite soil layer is required.
c) The rubber ring has great influence on soil-structure interaction model test on shaking tables. It is important to reasonably choose the elastic parameter and width of the rubber ring. The simulation results provide useful information for this purpose.

Acknowledgements

This work described in this paper was supported by a grant from City University of Hong Kong (Project No. 7001591).

References

Anandarajah, A., Rashidi, H. and Arulanandan, K. (1995), "Elasto-plastic finite element analyses of a soil-structure system under earthquake excitations", *Computers and Geotechnics*, **17**, 301-325.

Aviles, J. and Suarez, M. (2002), "Effective periods and damping of building-foundation systems including seismic wave effects", *Eng. Struct.*, **24**, 553-562.

Dominguez, J. (1978), "Dynamic stiffness of rectangular foundation", Report No.R78-20, Dept. of Civil Engineering, MIT

Genes, M.C. and Kocak, S.A. (2002), "Combined element based soil-structure interaction model for large-scale systems and applications on parallel platforms", *Eng. Struct.*, **24**, 1119-1131.

Huang, W.X., Bauer, E. and Sloan, S.W. (2003), "Behaviour of interfacial layer along granular soil-structure", *Struct. Eng. Mech.*, **15**(3), 315-329.

Kocak, S. and Mengi, Y.A. (2000), "Simple soil-structure interaction model", *Applied Mathematical Modelling*, **24**, 607-635.

Li, Q.S., Fang, J.Q. and Jeary, A.P. (1998), "Calculation of vertical dynamic characteristics of tall buildings with viscous damping", *Int. J. Solid Struct.*, **35**(24), 3165-3176.

Liao, Z.P. (1987), "Studies on the artificial boundary in the transient elastic wave analysis", *Earthquake Engineering and Engineering Vibration*, **7**(3), 12-23. (in Chinese)

Liu, J., Xiao, H.B., Tang, J. and Li, Q.S. (2004), "Analysis of load-transfer of single pile in layered soils", *Computer and Geotechnics*, **31**, 127-135.

Lou, M.L. and Lin, G. (1986), "Wave reflection effect of the artificial boundary in the viscoelastic soil foundation", *J. of Hydraulic Engineering*, **6**, 20-30. (in Chinese)

Lou, M.L., Wang, W.J., Zhu, T. and Ma, H.C. (2000), "Soil lateral boundary effect in shaking table model test of

soil-structure system", *Earthquake Engineering and Engineering Vibration*, **20**(4), 30-36. (in Chinese)
Lysmer, J. and Kulemeyer, R.L. (1969), "Finite dynamic model for infinite media", *J. Eng. Mech.*, ASCE, **95**, 759-877.
Wolf, J.P. (1985), *Dynamic Soil-Structure Interaction,* Prentice-Hall Inc., Englewood Cliffs, N. J.
Zhang, C. (1991), "Infinite boundary elements for dynamic problems of 3-D halfspace", *Int. J. Num. Meth. Eng.*, **30**, 447-462.